Eur. Phys. J. B **16**, 501–505 (2000)

THE EUROPEAN PHYSICAL JOURNAL B

EDP Sciences

Growth exponent in the Domany-Kinzel cellular automaton

A.P.F. Atman[a] and J.G. Moreira[b]

Departamento de Física, Instituto de Ciências Exatas, Universidade Federal de Minas Gerais, CP 702, 30123-970, Belo Horizonte, MG - Brazil

Received 15 March 2000

Abstract. In a roughening process, the growth exponent β describes how the roughness w grows with the time t: $w \sim t^{\beta}$. We determine the exponent β of a growth process generated by the spatiotemporal patterns of the one-dimensional Domany-Kinzel cellular automaton. The values obtained for β show a cusp at the frozen/active transition which permits determination of the transition line. The β value at the transition depends on the scheme used: symmetric ($\beta \simeq 0.83$) or non-symmetric ($\beta \simeq 0.61$). Using damage spreading ideas, we also determine the active/chaotic transition line; this line depends on how the replicas are updated.

PACS. 05.10.-a Computational methods in statistical physics and nonlinear dynamics – 02.50.-r Probability theory, stochastic processes, and statistics

1 Introduction

The one-dimensional Domany-Kinzel cellular automaton (DKCA) is a totally discrete systems – temporally, spatially and in numbers of states – with several applications in physics, chemistry, biology, computer science, etc. The DKCA phase diagram was originally proposed by Domany and Kinzel [1] who showed the existence of two phases: an active phase and a frozen one. A more detailed study, using numerical simulation, was present by Martins *et al.* [2], where a new phase in the active region – a chaotic phase – was discovered using the damage spreading technique. Further, Zebende and Penna [3] used the gradient method to determine the phase boundaries with high precision. Recently, Tomé [4] explored some details of the joint evolution of two DKCA. She considered the problem of simultaneous updating of two replicas using pseudo-random numbers; two prescriptions were presented for the joint evolution: one used by Martins *et al.* [2] and another introduced by Kohring and Schreckenberg [5]. Hinrichsen *et al.* [6] discovered a third phase in the DKCA diagram, using a thorough analysis of the damage spreading technique to split the active phase into three different regions: a chaotic region, where the damage spreads for every member of this family of dynamic procedures; an active region, where the damage heals for every member of this family, and another active region, where the damage spreads for a subset of the possible dynamic procedures and heals for the others. This new phase was obtained with a prescription that updates the replicas using the minimal correlations.

[a] e-mail: atman@fisica.ufmg.br
[b] e-mail: jmoreira@ipe.fisica.ufmg.br

In 1997, de Sales *et al.* [7] showed that the roughness exponent α can be used to classify the deterministic cellular automata (CA) described by Wolfram [8]. More recently [9], they showed that this exponent also can be used to detect the frozen/active transition in DKCA directly from the automata, without reference to order parameters or response functions. This method also can be used to detect phase transitions in another kind of model, such as the Potts model [10]. Beyond the roughness exponent α, the growth exponent β is another critical exponent used to describe various roughening processes in the surface growth context [11,12].

In this work, we introduce the growth exponent method to identify phase transitions. We apply this method to the one-dimensional DKCA to detect the phase transitions directly from the automata and build the DKCA phase diagram. To obtain self-affine rough profiles, we use the accumulation method to perform a mapping to the solid-on-solid (SOS) model, and measure the time evolution of the roughness of the interface to obtain the exponent β. In the frozen/active transition, the exponent β has a maximum, and two schemes are used to update the system [13]: a symmetric scheme, that corresponds to a triangular lattice, and a nonsymmetric scheme. In the symmetric scheme we obtain $\beta \simeq 0.83$, consistent with the directed percolation (DP) prediction; but in the nonsymmetric scheme, $\beta \simeq 0.61$, an unusual value that was not expected. It is expected [13], rather, to find the same value for β in the two schemes.

Very recently, a quite similar method was used by Lauritsen and Alava [14], to study the Edwards-Wilkinson equation with columnar noise, and by Dickman [15], to study the contact process.

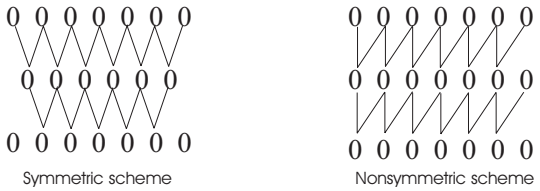

Fig. 1. Schemes used to update the systems.

This studies do not consider damage spreading, and cannot detect the chaotic/non-chaotic transition. To evidence this transition, we use the damage spreading ideas [16]: the difference between two replicas, which evolve with same dynamics, is used to perform the same SOS mapping as mentioned above, *via* the accumulation method. We use three different prescriptions for the simultaneous updating of the replicas and obtain three different transition lines.

In Section 2, we introduce the growth exponent method and show the results obtained for the frozen/active transition. The damage spreading ideas and the chaotic/non-chaotic transition are presented in the Section 3. Finally, we let to the Section 4 our conclusions and acknowledgments.

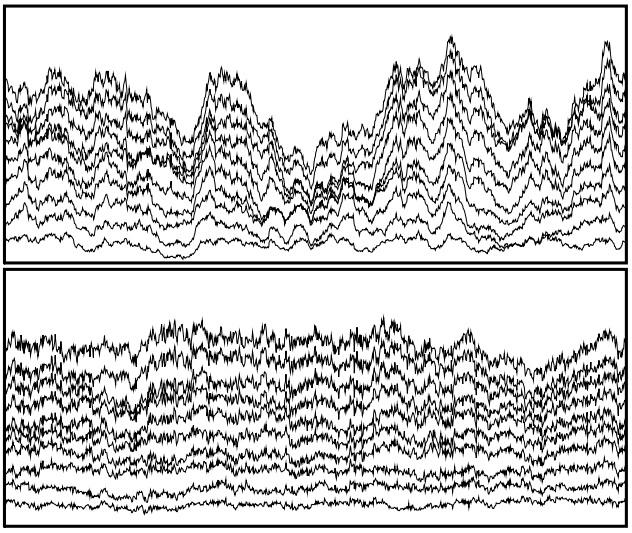

Fig. 2. Evolution of profiles generated by the accumulation method. Above: profiles generated in the symmetric scheme on a lattice with $L = 1\,000$. Below: profiles generated in the nonsymmetric scheme, $L = 1\,000$. Both figures have the same initial profile and same sequence of random noise, and the profiles were taken at the same instants of time in both schemes. Each profile was taken after 1 000 time steps.

2 Frozen-active transition

The DKCA consists of a linear chain of L sites ($i = 1, 2, ..., L$), with periodic boundary conditions, where each site has two possible states $\sigma = 0, 1$ (frozen, active). The state of the system at time t is given by the set $\{\sigma_i\}$. In contrast to the deterministic CA studied by Wolfram [8], the DKCA is probabilistic, in the sense that the rules that update the system are given by conditional probabilities, $P(\sigma_{i-1}(t), \sigma_{i+1}(t)|\sigma_i(t+1))$ (in the symmetric scheme). That is, the state of a given site in time $(t+1)$ depends, in a probabilistic fashion, upon the state of the two nearest neighbours at time t. In the DKCA, the conditional probabilities in the isotropic case are

$$\begin{aligned} &P(0,1|1) = P(1,0|1) = p_1, \\ &P(1,1|1) = p_2, \\ &P(0,0|1) = 0. \end{aligned}$$

Obviously,

$$P(\sigma_{i-1}, \sigma_{i+1}|0) = 1 - P(\sigma_{i-1}, \sigma_{i+1}|1).$$

In the nonsymmetric scheme, the state of a given site in time $(t+1)$ depends upon the state of itself and of the one nearest neighbour, both at time t. Then, the conditional probabilities are given by $P(\sigma_{i-1}(t), \sigma_i(t)|\sigma_i(t+1))$, and $P(\sigma_{i-1}, \sigma_i|0) = 1 - P(\sigma_{i-1}, \sigma_i|1)$. The values of the conditional probabilities are the same in both schemes. In Figure 1 we reproduce a representation of these schemes.

Depending on the values of the parameters (p_1, p_2), the asymptotic $(t \to \infty)$ state of the system is either a frozen state, with all sites in state 0, or has a finite fraction of sites with value 1, the active state. This is a second order phase transition, characterized by universal critical exponents [1].

To study the phase diagram of the DKCA, we use the accumulation method, utilized by Sales *et al.* [9], to obtain profiles in analogy with solid-on-solid (SOS) models in (1+1) dimensions. A similar method was proposed by Kremer and Wolf [17] to measure the width of an interface in the presence of overhangs and holes. This method consists in accumulating (or summing) all the values assumed by the variables $\sigma_i(t)$ during a given number t of successive time steps

$$h_i(t) = \sum_{\tau=0}^{t} \sigma_i(\tau). \tag{1}$$

The differences between the schemes become explicit at this point. In the Figure 2, we can observe several profiles at criticality in both schemes, generated after we apply the accumulation method. It is evident that different schemes lead to completely different profiles.

Thus, we obtain growth processes, the nature of whose correlations can be investigated through the analysis of the roughness $w(L,t)$ [11]. The roughness is defined by

$$w^2(L,t) = \frac{1}{L} \sum_{i=1}^{L} \left(h_i(t) - \overline{h}(t)\right)^2, \tag{2}$$

where $\overline{h}(t)$ is the mean value of $h_i(t)$ at time t. In fact, in order to consider the initial roughness of the profiles,

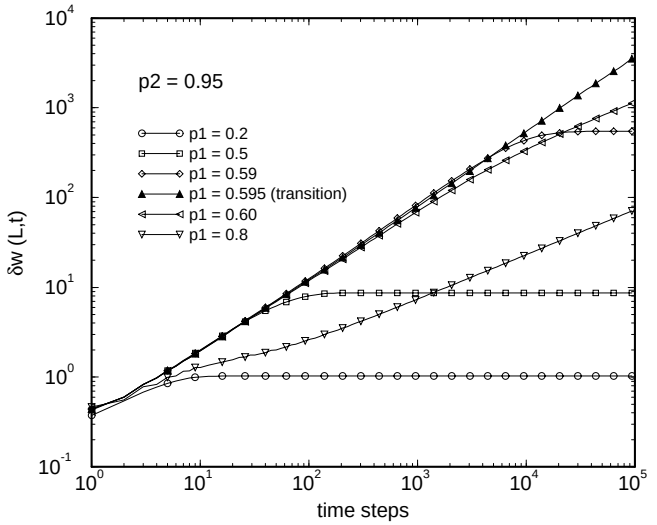

Fig. 3. Evolution of the fluctuation in roughness $\delta w(L,t)$ with time t in a log-log plot, for $p_2 = 0.95$ and five different values of p_1. We use $L = 10\,000$ and 50 samples. Note that the frozen/active transition occurs when the roughness grows indefinitely ($p_1 = 0.595$ - filled symbols).

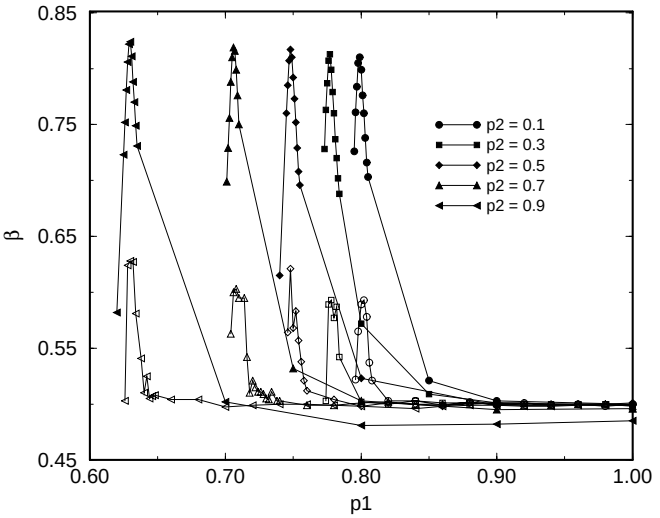

Fig. 4. Evolution of growth exponent β as a function of p_1, in the frozen/active transition, in the two updating schemes; the system has $L = 10\,000$. Five different values of p_2 are shown. The maximum of β indicates the transition. The symmetric scheme is represented by filled symbols and the nonsymmetric scheme by open symbols. The lines are to guide the eye.

we work with the fluctuation in roughness [18]

$$\delta w(L,t) = \sqrt{w^2(L,t) - w^2(L,0)}. \tag{3}$$

We expect that the behaviour of $\delta w(L,t)$ has the form

$$\delta w(L,t) = L^{\alpha} f\left(\frac{t}{L^z}\right), \tag{4}$$

where $f(u)$ is a universal scaling function, α is the roughness exponent, $z = (\alpha/\beta)$ is the dynamic exponent and β is the growth exponent. The function $f(u) =$ const. at large times ($t \gg L^z$) and $f(u) \sim u^{\beta}$ at short times ($t \ll L^z$). So, at short times, we expect that $\delta w(L,t) \sim t^{\beta}$ and can measure β calculating the slope of the log-log plot of $\delta w(L,t)$ *versus* t. The growth exponent denotes how the profile roughness grows with time: $\beta = 1/2$ means that the profile is not correlated, and is analogous to that generated by random deposition [11]; if $\beta > 1/2$, the profile tends to grow more at the tips, which causes the roughness increases faster, in contrast to $\beta < 1/2$, where the valleys grows quickly and make the roughness increase more slowly.

Typical results for the evolution of the roughness are shown in Figure 3. These results correspond to averages over 50 random initial configurations taken after 100 000 time steps in DKCA containing $L = 10\,000$ sites. Each curve in this graph (101 points) takes approximately one hour of CPU time on a Digital 500au workstation. We can observe that the roughness reaches the steady state in the frozen phase and grows indefinitely in the active phase. The values of β at the transition are shown in Figure 4, for both schemes. The exponent β is measured over more than three decades ($10 < t < 100\,000$ and $0.1 < \delta w < 1\,000$). Note that β shows a maximum at the transition and tends to the value $\beta = 1/2$ quickly after the transition, remaining at this value until $p_1 = 1$. The value of the β exponent at the transition depends of the scheme utilized in the DKCA. Nagy *et al.* [13] describe two schemes: a symmetric one, where the even (odd) sites are updated at even (odd) times; and a nonsymmetric one, where all sites are updated at each time step, but the neighbours of site $(i, t+1)$ are $(i-1, t)$ and (i, t). The symmetric scheme has been used in most previous studies of the model. In the symmetric scheme, we find $\beta = 0.81(2)$, compatible with the universality class of directed percolation (DP) ($\beta \simeq 0.84$) [15]. In the nonsymmetric scheme, we find $\beta = 0.61(2)$, clearly different from the DP value.

A finite size scaling analysis was made for the exponent β and shows that the width of the peak vanishes when the size of system goes to infinity. The value of the exponent β when the system size goes to infinity approaches $\beta \simeq 0.83(2)$ at the frozen/active transition in the symmetric scheme, and is valid for all values of $p_2 \neq 1$.

On the line $p_2 = 1$, the system is mapped onto the two-dimensional Ising model [19], and the β value is significant greater in the two schemes: $\beta = 0.99(1)$ in the symmetric, and $\beta = 0.75(1)$ in the nonsymmetric. The value in the symmetric scheme agrees with the literature [6], which predicts that all points on the phase boundary, except the line $p_2 = 1$, are characterized by directed percolation (DP) exponents. On the line $p_2 = 1$, the model has been solved exactly, and can be mapped onto the two-dimensional Ising model universality class, which leads to the value $\beta = 1$ [1].

The value $\beta > 1/2$ denotes the trend of the system to grow faster at the tips which can be understood as a preservation of active sites. At the transition, few sites remain active, which causes $h_i(t)$ to grow only near

active sites, contributing to an increase in the roughness. In the active phase, many sites are active, but uncorrelated, randomly increasing the height $h_i(t)$, so that $\beta = 1/2$.

The roughness exponent is defined only in the frozen phase because, in the active phase, the steady state is not reached. We calculate the Hurst exponent, H, very close to the transition and find, in the symmetric scheme, $H = 0.61(2)$. As noted by de Sales *et al.* [9] , there is a maximum in the H exponent, marking the phase transition. In the nonsymmetric scheme, the value of H at the transition is much smaller, $\alpha \simeq 0.25$, and the maximum is not very clear.

3 Active-chaotic transition

Martins *et al.* [2] used the damage spreading technique to show that the active phase of DKCA can be split into two phases, chaotic and non-chaotic. The order parameter of this transition is the difference between two replicas with slightly different initial configurations. They let the system evolve until it attains equilibrium, and then a replica of the automaton is created with some sites altered (damage). So the two replicas, one with states $\sigma_i(t)$ the another with states $\varrho_i(t)$, evolve with the same dynamics, and the difference between the automata

$$\Gamma_i(t) = |\sigma_i(t) - \varrho_i(t)|,$$

is measured. The fraction of sites in replica system that differ from their counterpart in the original system is called the Hamming distance, defined as

$$D_{\mathrm{H}}(t) = \frac{1}{L}\sum_i \Gamma_i(t).$$

The stationary Hamming distance is null in the non-chaotic phase and positive in the chaotic phase.

To obtain the chaotic/non-chaotic boundary, we use a slightly different method, where the difference between the two automata is used to perform the same mapping to a SOS model as we did in the accumulation method

$$h_i(t) = \sum_{\tau=0}^{t} \Gamma_i(\tau). \tag{5}$$

Thus, the profile generated by the difference of the two replicas behaves exactly as the profiles generated in the frozen/active boundary: the roughness reaches a stationary value in the non-chaotic phase and grows indefinitely in the chaotic phase. This behaviour can be understood if we note that the difference between the replicas vanishes in the non-chaotic phase, which implies no contribution to the height $h_i(t)$, and is positive in chaotic phase, which implies in a persistent contribution to the height. The β exponent again passes through a maximum at the chaotic/non-chaotic transition, and its value depends on the scheme utilized.

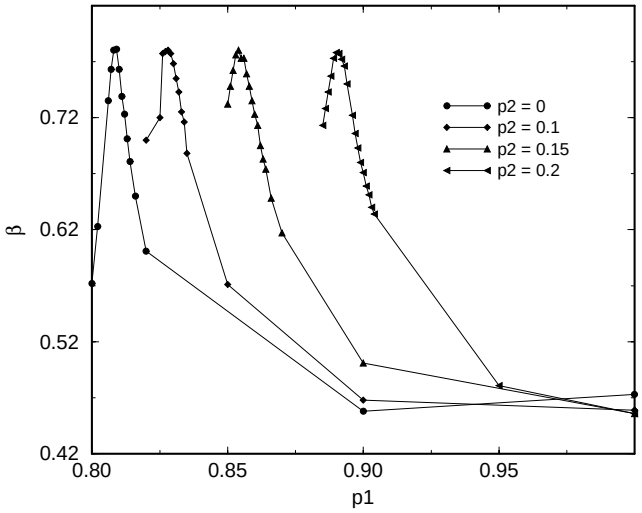

Fig. 5. Evolution of growth exponent β as a function of p_1, using damage spreading ideas to locate the chaotic/non-chaotic transition. The system has $L = 10\,000$. Four different values of p_2 are shown, for prescription A.

Figure 5 shows β for the chaotic/non-chaotic transitions, in the symmetric scheme. To obtain this figure, we use an automaton with $L = 10\,000$ and let it evolve for 10^4 time steps, at which time we create a replica of the system with an "initial damage", by flipping a fraction of the sites ($\sim 10\%$). Then the replicas evolve with the same dynamics during the 10^5 time steps, and the difference between them is measured as a function of time. An average over 50 realizations of initial damage was used.

We can locate the chaotic/non-chaotic phase transition, with the damage method, either waiting or not waiting for the original system to reach the steady state (first 10^4 time steps). The only difference we note is that the value for the exponent β, at the frozen/active transition, is more precise and the cusp is more pronounced if we wait the original to reach the steady state. For the chaotic/non-chaotic transition we obtain the same values with the two procedures, considering the statistical fluctuations.

At this point we have to emphasize the question of the dynamics of joint evolution of two CA's. Tomé [4] studied this joint evolution and showed that the CA's can evolve following two different prescriptions: prescription A, used by Martins *et al.* [2], which corresponds to updating both automata always using the same random number, and prescription B, introduced by Kohring and Schreckenberg [5], which implies that one must sometimes use two different random numbers (z_1 and z_2) to update the original and the replica. The later occurs when we have $(\sigma_{i-1} + \sigma_{i+1}) = 1$ and $(\varrho_{i-1} + \varrho_{i+1}) = 2$, or *vice-versa*. We make simulations using these two prescriptions and verify that there are significant differences in the chaotic/non-chaotic boundary of the DKCA $p_2 - p_1$ phase diagram, as shown in Figure 6. These differences were discovered by Bagnoli [20], who studied the damage spreading transition in the DKCA using a mean-field approximation; this work confirms his prediction numerically.

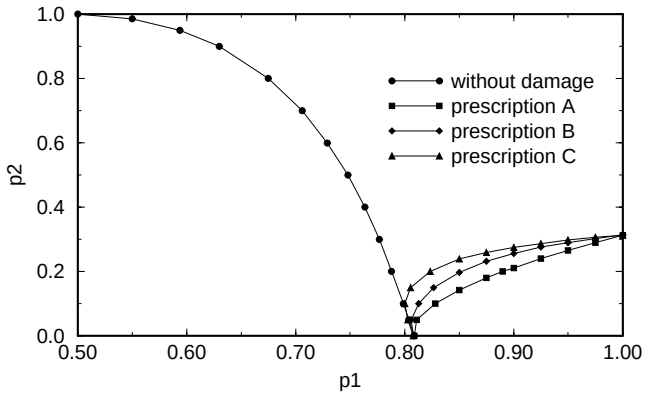

Fig. 6. DKCA $p_1 - p_2$ phase diagram obtained *via* the growth exponent method. Note that the three prescriptions yield different boundaries for the chaotic/non-chaotic transition. At $p_2 = 0$ we have $p_{1c} = 0.809(1)$ and at $p_1 = 1$ we have $p_{2c} = 0.3135(10)$, with all boundaries meeting at these points.

The frozen/active transition line and the chaotic/non-chaotic transition line obtained with prescription A are very close to the the phase diagram found by Zebende and Penna [3].

In this phase diagram we also present a third prescription, C, in which three random numbers, z_1, z_2 and z_3, are used to update the system. Defining

$$U_i = \sigma_{i-1} + 2\sigma_{i+1}$$

and

$$V_i = \varrho_{i-1} + 2\varrho_{i+1},$$

we have the following cases:
• if $U_i = V_i \ \rightarrow$ we use the same random number (z_1) to update the original and the replica;
• if $U_i = 1$ and $V_i = 2$ (or *vice-versa*) $\rightarrow$ we use z_1 for the original and z_2 for the replica;
• if $U_i = 1$ and $V_i = 3$ (or *vice-versa*) $\rightarrow$ we use z_1 for the original and z_3 for the replica.
• if $U_i = 2$ and $V_i = 3$ (or *vice-versa*) $\rightarrow$ we use z_2 for the original and z_3 for the replica.

To this prescription, the boundary is slighting above that of prescription B.

The difference between the phase boundaries appears to be due the different prescriptions for updating the systems in the damage spreading technique employed to detect the chaotic/non-chaotic transition: prescription A corresponds to maximal correlations between the random numbers; prescription B, to lower correlations, and prescription C to minimal correlations [6, 20]. We perform simulations using the third prescription in an attempt to reveal the third phase transition, reported by Hinrichsen *et al.* [6], but are unable to detect that transition using prescription C, which is the prescription with minimal correlations.

4 Conclusions

In this work we propose a new method to obtain the phase diagram of the DKCA using the growth exponent β, and detect the frozen/active boundary. At the transition, the values of the exponent β depend on the scheme used to update the system: $\beta = 0.83(2)$ for the symmetric scheme, and $\beta = 0.61(2)$ to the nonsymmetric scheme. Next, we extend this method, using damage spreading, to obtain the chaotic/non-chaotic boundary. Finally, we study three different prescriptions for the joint evolution of two DKCA's and construct the phase diagram, shown in Figure 6.

The advantage of this method to determine the phase diagram of the DKCA is that we do not need to wait for the system to reach the steady state, as in the methods used by Martins *et al.* [2] and Zebende and Penna [3], thereby economizing computation time. In addition, the growth exponent method can detect the chaotic/non-chaotic boundary much more clearly than the usual Hamming distance, which presents large fluctuations at the transition. This method can also be employed to detect phase transitions in other models where the accumulation process can be used [10].

The authors are indebted to M.L. Martins, T.J.P. Penna and R. Dickman for fruitful discussions and suggestions. We also thank R. Dickman for helpful criticism of the manuscript. This work is supported by Brazilian agencies CNPq and Fapemig.

References

1. E. Domany, W. Kinzel, Phys. Rev. Lett. **53**, 447 (1984).
2. M.L. Martins, H.F. Verona de Resende, C. Tsallis, A.C.N. de Magalhães, Phys. Rev. Lett. **66**, 2045 (1991).
3. G.F. Zebende, T.J.P. Penna, J. Stat. Phys. **74**, 1273 (1994).
4. T. Tomé, Physica A **212**, 99 (1992); E.P. Gheuvoghlanian, T. Tomé, Int. J. Mod. Phys. B **10**, 1245 (1997).
5. G.A. Kohring, M. Schreckenberg, J. Phys. I France **2**, 2033 (1992).
6. H. Hinrichsen, J.S. Weitz, E. Domany, J. Stat. Phys. **88**, 617 (1997).
7. J.A. de Sales, M.L. Martins, J.G. Moreira, Physica A **245**, 461 (1997).
8. S. Wolfram, *Theory and Applications of Cellular Automata* (Word Scientific, Singapore, 1986).
9. J.A. de Sales, M.L. Martins, J.G. Moreira, J. Phys. A **32**, 885 (1999).
10. J.A. Redinz, M.L. Martins (to be published).
11. A.-L. Barabási, H.E. Stanley, *Fractal Concepts in Surface Growth* (Cambridge Univ. Press, Cambridge, 1995).
12. P. Meakin, *Fractals, Scaling and Growth far from Equilibrium* (Cambridge Univ. Press, Cambridge, UK, 1998).
13. T.F. Nagy, S.D. Mahanti, C. Tsallis, Physica A **250**, 345 (1998).
14. K.B. Lauritsen, M. Alava, e-print: `cond-mat/9903346`.
15. R. Dickman, M.A. Muñoz, e-print: `cond-mat/0003480`.
16. H.J. Herrmann, Physica A **168**, 516 (1990).
17. S. Kremer, D.E. Wolf, Physica A **182**, 542 (1992).
18. T.J. da Silva, J.G. Moreira, Phys. Rev. E **56**, 4880 (1997).
19. W. Kinzel, Z. Phys. B **58**, 229-244 (1985).
20. F. Bagnoli, J. Stat. Phys. **85**, 151 (1996).